Bone 107 (2018) 78–87

Contents lists available at ScienceDirect

Bone

journal homepage: www.elsevier.com/locate/bone

Full Length Article

Bone marrow mechanotransduction in porcine explants alters kinase activation and enhances trabecular bone formation in the absence of osteocyte signaling

Kimberly J. Curtis [a,b], Thomas R. Coughlin [a,b], Devon E. Mason [b], Joel D. Boerckel [b], Glen L. Niebur [a,b,*]

[a] Tissue Mechanics Laboratory, University of Notre Dame, IN, 46556, USA
[b] Bioengineering Graduate Program, University of Notre Dame, IN, 46556, USA

ARTICLE INFO

Article history:
Received 12 September 2017
Revised 10 November 2017
Accepted 13 November 2017
Available online 14 November 2017

Keywords:
Mechanobiology
Bone marrow
Bone adaptation
Trabecular bone
Osteocytes
Dynamic histomorphometry

ABSTRACT

Bone is a dynamic tissue that can adapt its architecture in response to mechanical signals under the control of osteocytes, which sense mechanical deformation of the mineralized bone. However, cells in the marrow are also mechanosensitive and may contribute to load-induced bone adaptation, as marrow is subjected to mechanical stress during bone deformation. We investigated the contribution of mechanotransduction in marrow cells to trabecular bone formation by applying low magnitude mechanical stimulation (LMMS) to porcine vertebral trabecular bone explants in an *in situ* bioreactor. The bone formation rate was higher in stimulated explants compared to unloaded controls which represent a disuse condition (CNT). However, sclerostin protein expression in osteocytes was not different between groups, nor was expression of osteocytic mechanoregulatory genes SOST, IGF-1, CTGF, and Cyr61, suggesting the mechanoregulatory program of osteocytes was unaffected by the loading regime. In contrast, c-Fos, a gene indicative of mechanical stimulation, was upregulated in the marrow cells of mechanically stimulated explants, while the level of activated c-Jun decreased by 25%. The activator protein 1 (AP-1) transcription factor is a heterodimer of c-Fos and c-Jun, which led us to investigate the expression of the downstream target gene cyclin-D1, a gene associated with cell cycle progression and osteogenesis. Cyclin-D1 gene expression in the stimulated marrow was approximately double that of the controls. The level of phosphorylated PYK2, a purported inhibitor of osteoblast differentiation, also decreased in marrow cells from stimulated explants. Taken together, mechanotransduction in marrow cells induced trabecular bone formation independent of osteocyte signaling. Identifying the specific cells and signaling pathways involved, and verifying them with inhibition of specific signaling molecules, could lead to potential therapeutic targets for diseases characterized by bone loss.

1. Introduction

Bone adapts its shape and internal structure to the mechanical loads it encounters, a phenomenon observed, although not explained, by Wolff over 125 years ago [1]. In the past 50 years, Wolff's original hypotheses have been bolstered by the mechanostat theory of modeling, remodeling, and tissue repair [2,3]. Many controlled experiments have since demonstrated that repetitive mechanical loading exceeding a threshold increases bone mass and alters macroscopic geometry and microstructure [4–9], while loading below a minimum threshold leads to bone resorption [5,8,10–13]. These studies and many others, have supported the mechanostat theory that bone adaptation is regulated by coordinated activities of the primary bone cells – osteoblasts, osteoclasts, and osteocytes – through a process termed cellular mechanotransduction [2,14].

Osteocytes are a key mechanosensory cell in bone. They are entombed in the mineralized matrix, where they can act as strain gauges to sense the mechanical loading as modulated by local mechanical properties of the bone tissue [15–17]. The signal is transduced by activation of pathways associated with membrane and cytoskeletal deformation. Mechanical deformation of osteocytes both *in vitro* and *in vivo* affects gene and protein expression associated with osteogenesis. For example, insulin like growth factor-1 (IGF-1) is upregulated in mechanically stimulated osteocytes [18]. *In vivo*, IGF-1 expressed by osteocytes also regulates bone growth during development [19]. Mechanical loading also decreases expression of the SOST gene and secretion of sclerostin [7], a protein that inhibits canonical Wnt signaling, leading to decreased osteoblastic bone formation [20]. Mice deficient of SOST exhibited increased bone mass, bone strength, osteoblast activity, and bone formation [21,22], while transgenic overexpression of SOST in

* Corresponding author at: Bioengineering Graduate Program, 147 Multidisciplinary Engineering Research, Notre Dame, IN 46556, USA.
E-mail address: gniebur@nd.edu (G.L. Niebur).

https://doi.org/10.1016/j.bone.2017.11.007
8756-3282/

mice led to osteopenia [23,24]. Additionally, the majority of human osteocytes mineralized in trabecular bone express sclerostin [25]. Osteocytes further regulate bone remodeling by expressing ligand of receptor-activator of nuclear factor κB (RANK-L) and osteoprotegerin (OPG), molecules that compete to bind RANK and act to promote or inhibit osteoclast activation, respectively [26–28].

While the role of osteocyte mechanotransduction in bone modeling, remodeling, and microdamage repair is well established, many other cells in the bone and marrow niche are mechanosensitive and may contribute to bone's response to mechanical loading. Mesenchymal stromal cells (MSCs), osteoprogenitors, and osteoblasts respond to fluid shear stress *in vitro* [29–31]. Cells of the hematopoietic lineage are also mechanosensitive. For example, gene expression in megakaryocytes is affected by mechanical loading of the mouse ulna *in vivo* [32].

Bone marrow is normally subjected to repetitive mechanical stress [33,34] that is transmitted to the resident cells [35] during whole bone loading. When such mechanical loads were applied directly to marrow explants, increased ossification was observed compared to unloaded explants [36–38]. A recent study in which marrow from Kif3a knockout mice was transplanted into wild-type mice verified that *in vivo* mechanical loading of whole bones is at least partly transduced in the marrow [39]. Further, a mouse model of caudal vertebra loading demonstrated that new bone formation was strongly correlated to marrow deformation [40]. However, it is not clear from these *in vivo* studies whether mechanotransduction within the marrow alone is sufficient to affect bone apposition, or if it is coupled to osteocyte signaling.

The intimate interaction of bone and marrow *in vivo* make differentiating the relative contributions of mechanical loads in the two tissues difficult. An *in situ* culture methodology employing inertial loading of the marrow with minimal concomitant strain in the bone tissue [41,42] may potentially separate mechanotransduction occurring in marrow cells from that in osteocytes. The objective of this study was to elucidate the role of mechanotransduction in the marrow cell population in mechanically stimulated trabecular bone formation. To achieve this, a bioreactor was used to culture porcine trabecular bone explants and subject the marrow cells to shear stress via low-magnitude mechanical stimulation (LMMS) and 1) the dependence of bone formation on mechanical stimulation was quantified; 2) the expression of both mechanoregulatory genes and proteins in osteocytes was measured to identify complementary effects; and 3) altered expression of genes and activated signaling proteins within the marrow was measured.

2. Methods

2.1. Tissue preparation and bioreactor culture

Trabecular bone explants were prepared and cultured in a bioreactor as described in [41]. Briefly, cylindrical explants 8 mm in diameter and 1 cm in height were excised from porcine cervical vertebrae (Martins Meats, Wakarusa, IN) using a low speed diamond tip core drill (Starlite Industries, PA). Average bone volume, trabecular thickness, trabecular spacing, and structural model index were measured by micro-CT before bioreactor culture (Table 1). In the bioreactor, explants were held firmly between PEEK platens and supplied with a continuous flow of explant growth media at a rate of 0.9 ml/min via a peristaltic pump (Fig. 1A). A total of 40 ml of media was supplied to each explant, with half the volume replaced twice per week. The media was composed of 89% high glucose Dulbecco's Modified Eagle's Medium (DMEM), 10% fetal bovine serum (FBS), 1% antibiotic/antimycotic (100 units/ml penicillin, 0.1 mg/ml streptomycin, and 0.25 μg/ml amphotericin B) and supplemented with 20 mM β-glycerol phosphate (β-GP) and 50 μM ascorbic acid-2-phosphate (AA2P).

Table 1
Average bone volume percentage (BV/TV), trabecular thickness (Tb. Th.), trabecular spacing (Tb. Sp.), and structural model index (SMI) for porcine trabecular bone explants measured by micro-CT before the 28 day bioreactor culture (Mean ± S.D.; $N = 8$ per group).

	CNT	LMMS
BV/TV (%)	32.45 ± 0.02	31.98 ± 0.02
Tb. Th. (mm)	0.145 ± 0.01	0.145 ± 0.01
Tb. Sp. (mm)	0.444 ± 0.04	0.437 ± 0.03
SMI	−0.425 ± 0.20	−0.361 ± 0.16

2.2. Long term bioreactor culture

To measure the effect of mechanical stimulation on bone formation, two groups of eight trabecular bone explants were prepared from five pigs as described above. Explants were cultured for 28 days (Fig. 1B). Explants in the LMMS group were subjected to vibration stimulation of 0.3 g at 50 Hz for two 30 min bouts, 5 days/week. Unloaded explants (CNT) represented a disuse condition and were cultured in the bioreactor without stimulation. Media was supplemented with 0.5 mM alizarin red and 0.5 mM xylenol orange for 24 h on day 6 and day 27 of culture, respectively, to label bone formation for dynamic histomorphometry.

2.3. CFU-F assays

At the end of the long-term culture, marrow was removed from four explants in each group by centrifugation at 3500 RCF followed by a 10 min incubation in trypsin, and another centrifugation at 3500 RCF which effectively extracted the marrow cells from the bone (see Supplementary figure). Marrow cells from four additional explants were collected on the day of harvest. The cells were resuspended in warm MSC growth media (89% low glucose DMEM, 10% FBS, 1% antibiotic/antimycotic).

CFU-F assays were performed in triplicate for each group to quantify mesenchymal lineage cells. Marrow cells were plated at a density of 100,000 cells/well in six-well plates and cultured with MSC growth media. The wells were fixed and stained with crystal violet after 12 days. Colonies were counted using ImageJ (NIH) to determine the number of colony forming cells in the marrow.

2.4. Tripotentiality assays

Tripotentiality assays were performed to verify that plastic adherent cells were capable of differentiating to the three primary mesenchymal phenotypes. Adipogenic, osteogenic, and chondrogenic differentiation assays were carried out as described previously [43], with some modifications. Briefly, adherent cells were expanded to passage four using MSC growth media. Cells were plated at low density (30,000 cells/well) for osteogenic assays. Osteogenesis was induced using growth media supplemented with 10 mM β-GP, 50 μM AA2P, and 100 nM dexamethasone and assayed at day 21 by staining with alizarin red (Sigma).

Cells were plated at 200,000 cells per well for adipogenic assays. Adipogenesis was induced using three induction-maintenance cycles. Induction media consisted of high glucose DMEM, 10% FBS, 1% AB/AM, 1 μM dexamethasone, 200 μM indomethacin, 500 μM 3-Isobutyl-1-methylxanthine, 1 mg/ml insulin and maintenance media consisted of high glucose DMEM, 10% FBS, 1% AB/AM with 1 mg/ml of insulin. At day 21, lipids were stained using Oil Red O (Sigma).

Chondrogenesis was assayed using pellets of 250,000 cells with low glucose DMEM, 1% AB/AM, 1 mM dexamethoasone, 5 mg/ml AA2P, 4 mg/ml L-Proline, 1.0 mg/ml insulin, 0.55 mg/ml transferrin, 0.5 μg/ml sodium selenite, and 10 ng/ml of transforming growth factor β-3. Chondrogenic assays were assessed after 21 days using Alcian blue to stain glycosaminoglycans (GAGs), indicative of chondrogenesis.

2.5. Histomorphometry

Dynamic histomorphometry was performed on thick sections prepared from the explants after 28 days of culture. Following removal of marrow, the explants were dehydrated and cleared in a vacuum

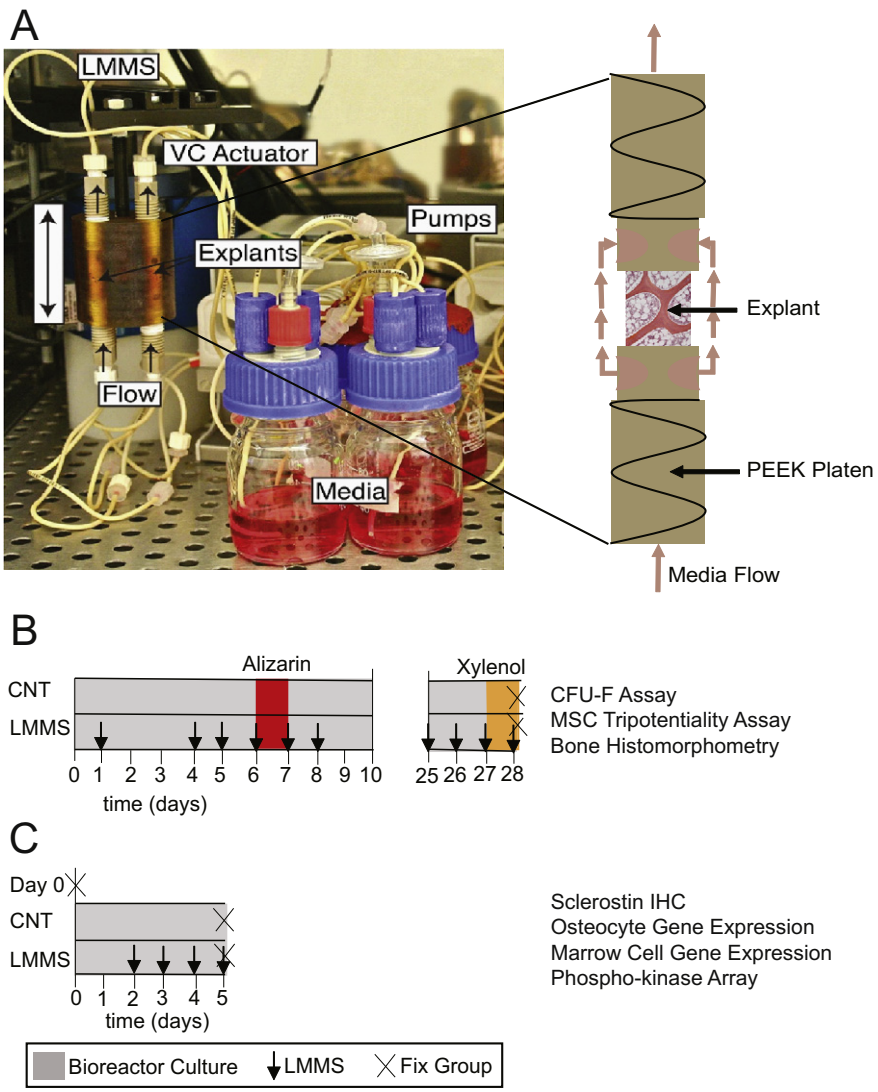

Fig. 1. (A) A voice coil linear actuator with sub-micron closed loop control applied LMMS to culture chambers. Accelerations were verified with an accelerometer. A peristaltic pump continuously circulated media from sample specific media reservoirs. Trabecular bone explants were held firmly between PEEK platens and were cultured in two experiments: long-term and short-term, where LMMS was applied at 0.3 g, 50 Hz for 30 min twice a day. Unstimulated explants were cultured in bioreactors without stimulation. (B) Explants were cultured for 28 days with (LMMS) and without stimulation (CNT). LMMS explants were subject to LMMS for 5 days/week for a total of twenty days. (C) In the short-term experiment, explants were cultured for five days in the unstimulated (CNT) and stimulated groups (LMMS) while the fresh explants (Day 0) were fixed on the day of slaughter. LMMS was applied on days 2 through 5.

chamber in ascending grades of ethanol (60%, 70%, 80%, 90%) for 2 h followed by 100% ethanol overnight and, finally, xylene overnight. They were then embedded in MMA (OsteoBed, Polysciences) in a vacuum chamber. Two consecutive 100 μm thick sections were cut from the center of each explant using a diamond wire saw, and mounted on microscope slides using Eukitt (Fluka). The mounted sections were polished using 600 grit polishing paper and descending grades of diamond pastes (30, 9, 3, 1, 0.25 μm). Two sections per sample were imaged to analyze a total tissue area of 30 mm^2 [44]. The outer 200 μm of the explant sections were not imaged to avoid measuring regions where fluid shear stress from the media occurs. Mineralizing surfaces and bone surfaces were measured using 100× magnification with an epifluorescent UV1A filter. Double labels were assessed at 100× magnification with an epifluorescent TRITC filter, which allowed both xylenol orange and alizarin red to be visualized. Percentage mineralizing bone surface (MS/BS), mineral apposition rate (MAR), bone formation rate (BFR), single labeled surface (sLS/BS), and double labeled surface (dLS/BS) were calculated for each explant and averaged within LMMS and CNT groups according to [44].

2.6. Immunohistochemistry for sclerostin

Short-term bioreactor culture was used to examine protein and gene expression (Fig. 1C). Three groups of eight explants (Day 0; CNT; LMMS) were excised from two pigs. Day 0 explants were fixed with 10% formalin on the day of slaughter for 48 h. CNT and LMMS explants were cultured for 5 days in bioreactors. LMMS explants were loaded twice/day at 50 Hz with 0.3 g acceleration for 30 mins on days 2 through 5 while CNT explants were unloaded. At the end of 5 days of culture, explants were fixed in neutral buffered formalin for 48 h, demineralized with 10% w/v EDTA, processed, paraffin embedded, and sectioned longitudinally at 6 μm for immunohistochemistry. Sections were dried at 60 °C, reacted for endogenous peroxidase activity, blocked, and incubated with anti-sclerostin primary antibody (Abcam). Secondary antibody labeling was achieved with the Vectastain Elite ABC kit (Vector Labs, Inc) with diaminobenzidine (DAB) as the chromogen. Nuclei were counterstained with methyl green. Two immuno-labeled sections from each sample were imaged at 500× and eight images were acquired per section for a total of sixteen images per sample. Osteocytes were

identified based on the presence of methyl green nuclear staining and osteocytes positive for sclerostin were identified based on the presence of DAB staining to quantify the percentage of sclerostin positive osteocytes.

2.7. Osteocyte gene expression

The short-term bioreactor experiment was repeated to measure mechanically induced gene expression in osteocytes. Three groups of eight explants were obtained from cervical vertebrae of four pigs (Day 0; CNT; LMMS), and RNA was isolated as described in [45]. Following culture, marrow was removed from the explants as described previously. Afterward, the bone explants were snap-frozen in liquid nitrogen and crushed with a mortar and pestle. TRIzol Reagent (Invitrogen) was added and the tissue was homogenized with a 20-gauge needle and syringe. The homogenized tissue solution was incubated with chloroform and then centrifuged. The supernatant containing RNA was decanted and added to an equal amount of 70% ethanol before being purified using RNeasy Mini Kits (Qiagen). RNA quantity and quality were measured with a spectrophotometer (NanoDrop). RNA was reverse transcribed to cDNA using the High Capacity cDNA Reverse Transcription Kit with RNase Inhibitor (Applied Biosystems). qPCR was carried out using iTaq Universal SYBR Green Supermix (Bio-Rad Laboratories, Inc.) on a CFX Connect Real-Time PCR Detection System (Bio-Rad). SOST, insulin-like growth factor-1 (IGF-1), osteoprotegerin (OPG), receptor activator of nuclear factor kappa-B ligand (RANKL), cysteine rich angiogenic inducer 61 (Cyr61), and connective tissue growth factor (CTGF) were amplified and standardized to Ribosomal Protein S2 (RPS2) using custom primer pairs based on RefSeq and Primer-BLAST data from the National Center for Biotechnology Information (Table 2). RPS2 was previously used as a reference gene in bone [46] and was confirmed to have approximately invariant C_T values. Data were analyzed using the $\Delta\Delta C_T$ method.

2.8. Marrow cell gene expression

A third short-term bioreactor experiment was performed to measure mechanically induced gene expression in marrow cells. Three groups of eight explants were obtained from cervical vertebrae of four pigs. Following 5 days of culture (Fig. 1C), marrow was removed from the explants by centrifugation at 3500 RCF as described above and filtered through a 40 μm cell filter to remove adipocytes. Eight million cells per explant were lysed and their RNA isolated and purified using RNeasy Mini Kit (Qiagen). RT-qPCR was performed as described above. c-FOS, IGF-1, cyclooxygenase 2 (COX-2), peroxisome proliferator activated receptor gamma (PPARγ), and cyclin-D1 were amplified and standardized to Ribosomal Protein S2 (RPS2) using custom primer pairs based on RefSeq and Primer-BLAST data from the National Center for Biotechnology Information (Table 2). RPS2 was confirmed to have approximately invariant C_T values. Data were analyzed using the $\Delta\Delta C_T$ method.

Table 2
Custom RT-qPCR primer sequences used for porcine cells generated with RefSeq from NCBI.

	Forward Primer (5′ to 3′)	Reverse Primer (5′ to 3′)
SOST	TCAAGAACGATGCCACGGAA	AGGCGTCTTTGGTCTCGAAG
IGF-1	ATCGTGGATGAGTGCTGCTT	ATGTACTTCCTTCTGAGCCTTGG
OPG	GTTCTGGAAACAGTGAATCGAC	CAGCAAACCTGAAGAACGCC
RANKL	CTCACGATCAACGCCACAGA	CGGTCATGATACCAGCAGGA
CTGF	ATACCGGGCTAAGTTCTGCG	GAACTCCACAGGAAGGGTGG
Cyr61	CACCAATGACAACCCCGACT	ACTTGGGCCGGTACTTCTTC
c-Fos	TCCTACTACCACTCACCGGC	CGTTGGGATGAAGTTGGCAC
COX-2	TGCGCCTTTTCAAGGATGGA	GTCTTTGGCTGTCGGAGGAT
PPARγ	CTATTCCATGCTGTCATGGGTG	ACCATGGTCACCTCTTGTGA
Cyclin-D1	TATTTGCATGACCCTGAGCTGG	ATCTAACCCTCCCCGCACAC
RPS2	CCACCTTTGACGCCATTTCC	CTCTGGTGTGGGTCTTCACA

2.9. Marrow protein expression

A Proteome Profiler Phospho-kinase Array (R&D Systems) was performed to measure kinase phosphorylation in marrow cells from eight (four LMMS and four CNT) of the same samples used for marrow cell gene expression following the manufacturer's protocol. Briefly, marrow was removed from LMMS and CNT explants after 5 days of bioreactor culture via centrifugation and the cells were filtered through a 40 μm filter to remove adipocytes. The remaining cells were lysed at a concentration of 10^7 cells/ml. The protein concentration was measured with a bicinchoninic acid (BCA) assay (Thermo Fisher), and 600 μg of protein per sample was incubated on membranes containing capture antibodies specific for 45 kinases related to the mitogen activated protein kinase (MAPK) signaling pathway (R&D Systems, Minneapolis). HRP-conjugated detection antibodies were added to the membranes, and the resulting chemiluminescence was visualized on a ChemiDoc-It Imager (UVP, Upland, CA).

2.10. Statistical analysis

For CFU-F assays and sclerostin immunohistochemistry, ANOVA was used to compare across LMMS, CNT, and Day 0 groups. A Student's *t*-test was used to compare histomorphometric parameters between LMMS and CNT groups. Gene expression data was analyzed with Wilcoxon signed rank tests, except for cyclin-D1 data, which was compared with a paired *t*-test. A one sample *t*-test was used to analyze the data from the phospho-kinase array.

3. Results

3.1. CFU-F assays and tripotentiality assays

Marrow cells retrieved from the explants that were cultured for 28 days formed adherent colonies. A smaller percentage of marrow cells formed colonies in explants cultured without mechanical stimulation (CNT) compared with fresh explants (Day 0) ($p = 0.02$), while explants cultured with mechanical stimulation (LMMS) were not different from CNT ($p = 0.06$) or Day 0 explants ($p = 0.74$) (Fig. 2A). MSCs expanded from the extracted marrow of both CNT and LMMS groups were positive for adipogenic, osteogenic, and chondrogenic differentiation when subjected to standard MSC differentiation protocols (Fig. 2B).

3.2. Histomorphometry

Double-labeled surfaces with both alizarin red and xylenol orange were observed in both CNT and LMMS groups, indicating active bone formation after 28 days of culture (Fig. 3A). The BFR was higher in LMMS explants compared to CNT explants (Fig. 3B; $p = 0.02$), while MAR ($p = 0.22$), mineralizing surface (Fig. 3C; $p = 0.33$), sLS/BS (Fig. 3D; $p = 0.936$), and dLS/BS (Fig. 3D; $p = 0.071$) were similar between the two groups (Table 3).

3.3. Osteocyte protein and gene expression

Sclerostin positive osteocytes were present in all explants cultured for 5 days. In total, 4783, 4280, and 4069 osteocytes were analyzed in Day 0, CNT, and LMMS explants, respectively. Approximately 75% of osteocytes were labeled positive for sclerostin in all groups ($p>0.8$; Fig. 4). Similarly, expression of SOST, IGF-1, RANKL/OPG, CTGF, and Cyr61 did not differ between LMMS and CNT groups (Fig. 4C; $p = 0.20$–0.95).

3.4. Marrow gene and protein expression

Marrow cells in the loaded explants cultured for 5 days expressed a higher level of c-Fos gene transcription than controls ($p<0.05$; Fig. 5). In

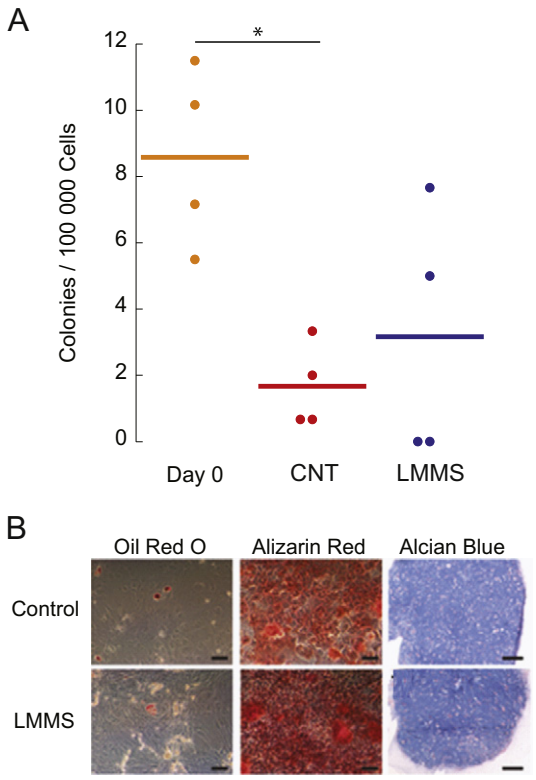

Fig. 2. (A) The percentage of marrow cells that formed colonies was lower in explants cultured without mechanical stimulation (CNT) than in Day 0 controls (ANOVA; $p = 0.02$). The percentage of colony-forming cells in explants cultured with mechanical stimulation (LMMS) was not statistically different from controls (ANOVA; Day 0 *vs.* LMMS $p = 0.06$, CNT *vs.* LMMS $p = 0.74$). (B) Representative images of adipogenic (Oil Red O), osteogenic (alizarin red), and chondrogenic assays (Alcian blue) for cells from both CNT and LMMS treated with standard differentiation media. Tripotentiality assays indicated that the plastic adherent cells in the explants were MSCs.

contrast, expression of IGF-1, COX-2, and PPARγ were not affected by loading ($p = 0.06$–1.00).

Levels of phosphorylated kinases were altered in mechanically stimulated marrow (Fig. 6). The levels of five phosphorylated kinases were lower in all four loaded samples compared to the controls. Three of these, c-Jun, p70 S6 kinase, and PYK2, demonstrated significantly lower expression in LMMS samples compared to CNT ($p<0.05$; Fig. 6B).

We further explored the dichotomous results of increased c-Fos mRNA and lower levels of phosphorylated c-Jun in the stimulated explants, as c-Jun and c-Fos dimerize to form the AP-1 transcription factor. When AP-1 is composed of c-Jun and c-Fos, it acts as a promoter of cyclin-D1, a key regulator of the cell cycle [47,48]. As such, we quantified cyclin-D1 mRNA expression from marrow cells in the same experiments. Cyclin-D1 expression was nearly two times higher in the marrow cells from the stimulated explants compared to the controls ($p<0.01$; Fig. 7).

Table 3
Histomorphometric parameters for the 28 days culture study (Mean ± S.D.; N = 8 per group).

	CNT	LMMS	*p*-value
BA/TA (%)	19.65 ± 3.09	18.88 ± 3.37	0.640
BS/TA (mm^{-1})	4.592 ± 1.43	4.544 ± 1.56	0.949
sLS/BS	0.390 ± 0.10	0.385 ± 0.11	0.936
dLS/BS	0.046 ± 0.03	0.095 ± 0.06	0.071
MS/BS	0.241 ± 0.07	0.287 ± 0.10	0.325
MAR (μm/day)	0.942 ± 0.21	1.07 ± 0.20	0.216
BFR ($\mu m^3/\mu m^2$/yr)	79.19 ± 15.4	107.06 ± 25.4	0.023

4. Discussion

While the importance of marrow as a source of bone progenitor cells has been accepted, and recently demonstrated [39], the osteocyte has been the main focus as the regulator of mechanical adaptation. We hypothesized that mechanotransduction in bone marrow cells can also affect bone adaptation. Mechanical stimulation applied to the marrow through LMMS enhanced bone formation in trabecular bone, although sclerostin expression in osteocytes, which is downregulated by mechanical loading [7], did not differ between groups at either the gene or protein level. Considering that sclerostin is one of the key regulatory proteins secreted by osteocytes [49,50], this indicates that the osteocytes were not responding to the mechanical stimulation. This was corroborated by the absence of changes in IGF-1 gene expression, which is one of the first genes to be upregulated by mechanical stimulation [18]. Indeed, compared to explants fixed immediately after harvest, RANKL/

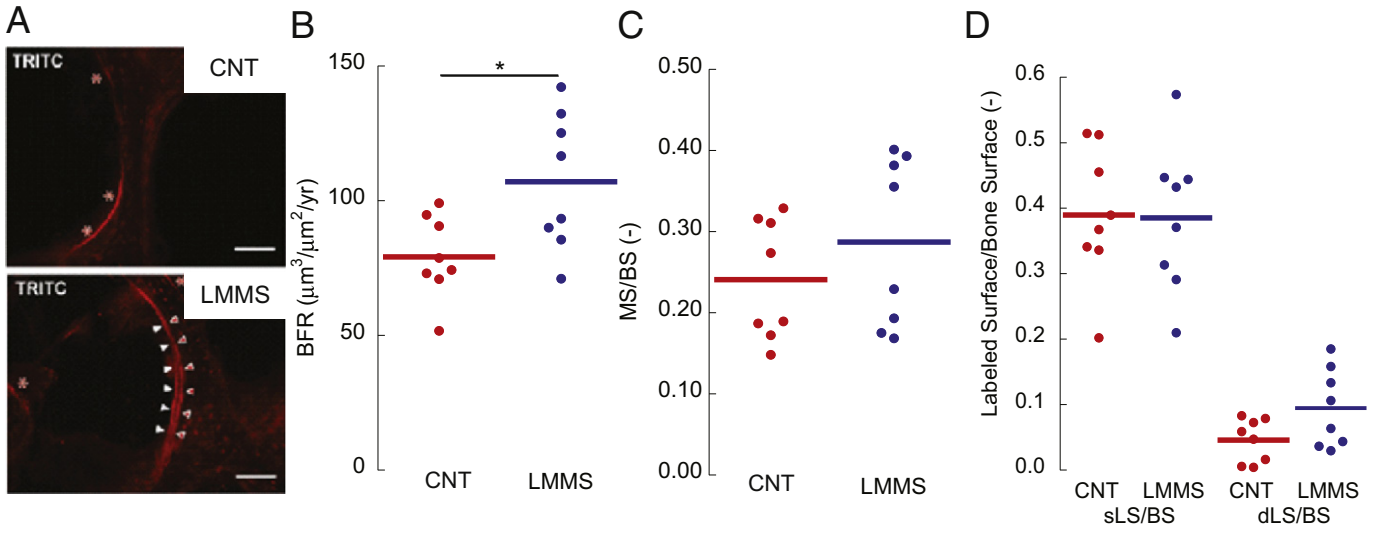

Fig. 3. (A) Representative fluorochrome labels in trabecular bone explants after 28 days of bioreactor culture. Explants were imaged using a UV1A filter (Nikon) to quantify mineralizing surfaces at 100× and TRITC to measure double labels at 200×. Asterisks indicate labeling with alizarin red or xylenol orange. Arrowheads indicate regions of double label. Scale bars are 100 μm. (B) BFR in explants cultured for 28 days with LMMS was significantly higher than explants without stimulation (CNT) (*$p = 0.023$). (C) Mineralizing surfaces were similar between groups ($p = 0.325$). (D) There was no difference in length of single labeled surfaces ($p = 0.936$) or double labeled surfaces ($p = 0.071$) between LMMS and CNT. Student's *t*-test was used to compare parameters between groups.

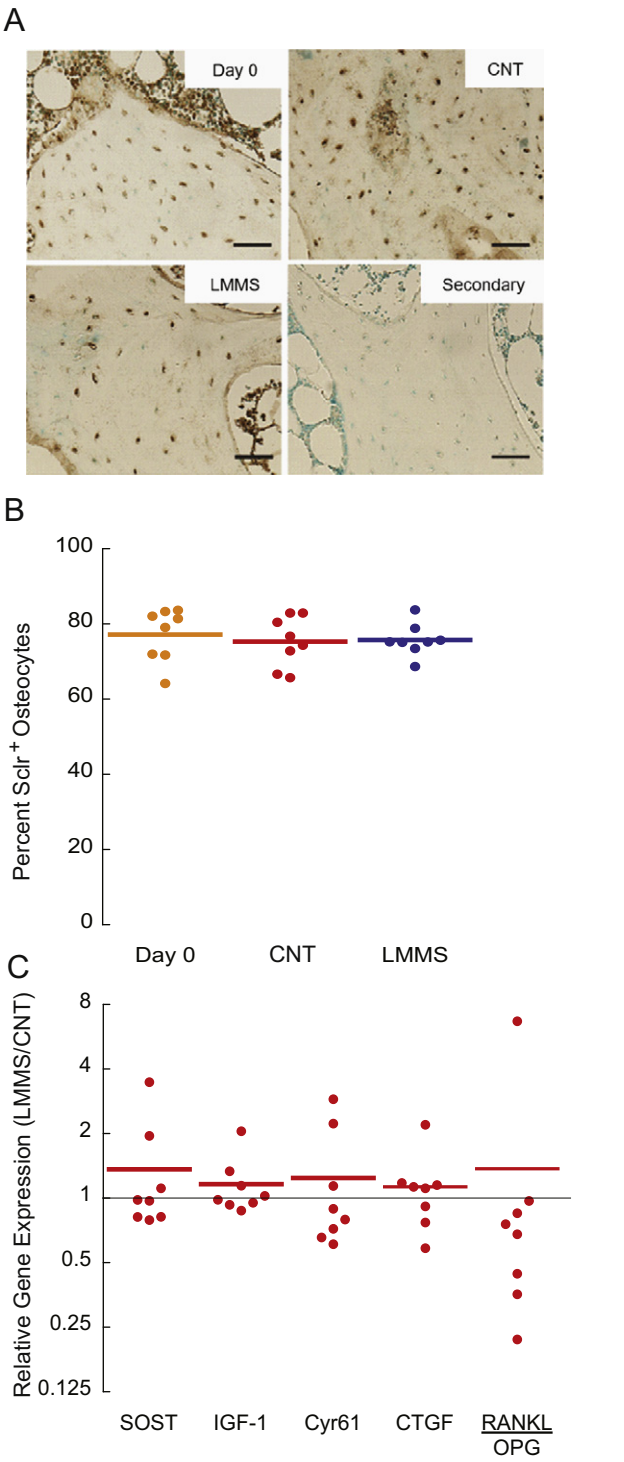

Fig. 4. (A) Representative immunohistochemistry staining for sclerostin using DAB chromogen (brown) and methyl green nuclear counterstain (green) for explants fixed on the day of slaughter (Day 0) and the explants cultured for 5 days (LMMS and CNT). Scale bar is 100 μm. (B) The percentage of osteocytes expressing sclerostin did not differ between fresh (Day 0), CNT, and LMMS groups ($p > 0.8$, ANOVA, $N = 8$ per group). (C) Expression of genes related to osteocyte mechanoregulation were not different between osteocytes from loaded and unloaded explants ($p > 0.20$, Wilcoxon signed rank). Each point represents the ratio of the expression in an LMMS sample to the mean of the CNT samples from the same animal.

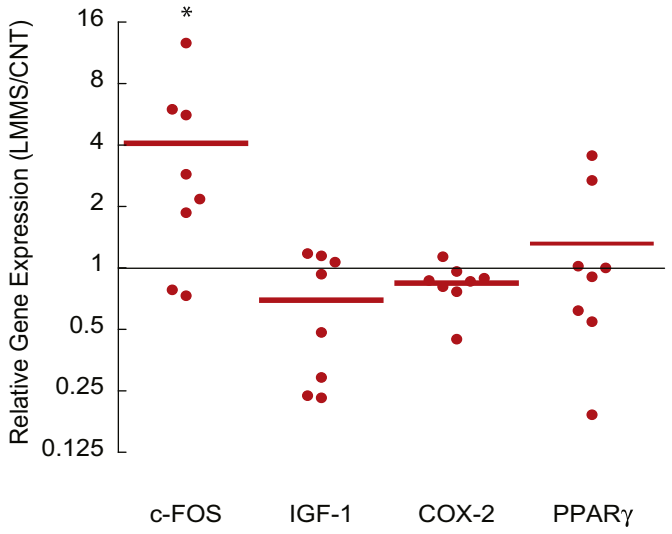

Fig. 5. c-Fos gene expression was higher in marrow cells from loaded explants compared to controls, while other genes associated with cell mechanotransduction were not altered by loading ($^*p < 0.05$, Wilcoxon signed rank). Each point represents the ratio of the expression in an LMMS sample to the mean of the CNT samples from the same animal.

OPG was upregulated 1.5 fold in osteocytes from the cultured explants (see Supplementary data), consistent with decreased mechanical stimulation during explant culture compared to *in vivo*. This is consistent with the negligible strain induced in the bone matrix by LMMS stimulation [51]. We verified that mechanical stimulation altered both gene expression and phosphorylated kinase levels in the marrow cells. Given the altered gene and protein responses in the marrow cells but not in osteocytes, we conclude that mechanotransduction in the marrow cell population was responsible for the greater bone formation. Hence, not only do marrow cells respond to mechanical loading, but they respond to the relatively small mean shear stress, on the order of 0.09 Pa, imparted by vibration [42,51]. In comparison, models of marrow shear stress induced by physiological bone loading suggest the shear stress exceeds 1.5 Pa [33,34]. MSCs have also been reported to sense acceleration in the range of magnitudes in this experiment [52]; however in our previous studies we found that the bone formation response is proportional to shear stress [41].

We used a phospho-kinase array to screen for potential pathways that could explain the increased bone formation in the stimulated explants. Since kinase activity can change rapidly, we harvested cells and transferred them to ice cold lysis buffer immediately after the last bout of stimulation. Following five days of culture, the relative levels of phosphorylated c-Jun, p70 S6 kinase, and proline-rich tyrosine kinase 2 (PYK2) were all significantly lower in mechanically stimulated bones. These proteins are associated with inflammation in immune cells, which make up approximately 40% of marrow cells [53], but may also play a role in differentiation of mesenchymal lineage cells. For example, trabecular bone formation is increased in PYK2 knockout mice, and marrow cells from these animals show significantly increased osteoblastic differentiation, alkaline phosphatase (ALP) production, and mineralization [54], suggesting that PYK2 is a negative regulator of osteoprogenitors [54,55]. However, the role of PYK2 phosphorylation in osteoblast differentiation is not fully clear, as phosphorylation inhibitors markedly increased osteogenic markers in some studies [56,57] while mutant PYK2 lacking kinase activity expressed in osteoblasts inhibited ALP production in another [54].

We assayed cyclin-D1 gene expression to assess a downstream target of AP-1, which is a heterodimer of c-Fos and c-Jun. Unexpectedly, cyclin-D1 gene expression increased, despite a decrease in activated c-Jun kinase in mechanically stimulated marrow. However, while N-terminal phosphorylation of c-Jun enhances cyclin-D1 expression, it is not necessary [58]. Constitutive phosphorylation of c-Jun doubles cyclin-D1 gene expression, while inhibiting c-Jun phosphorylation decreases it ten-fold [59]. Phosphorylated c-Jun levels in the stimulated explants only

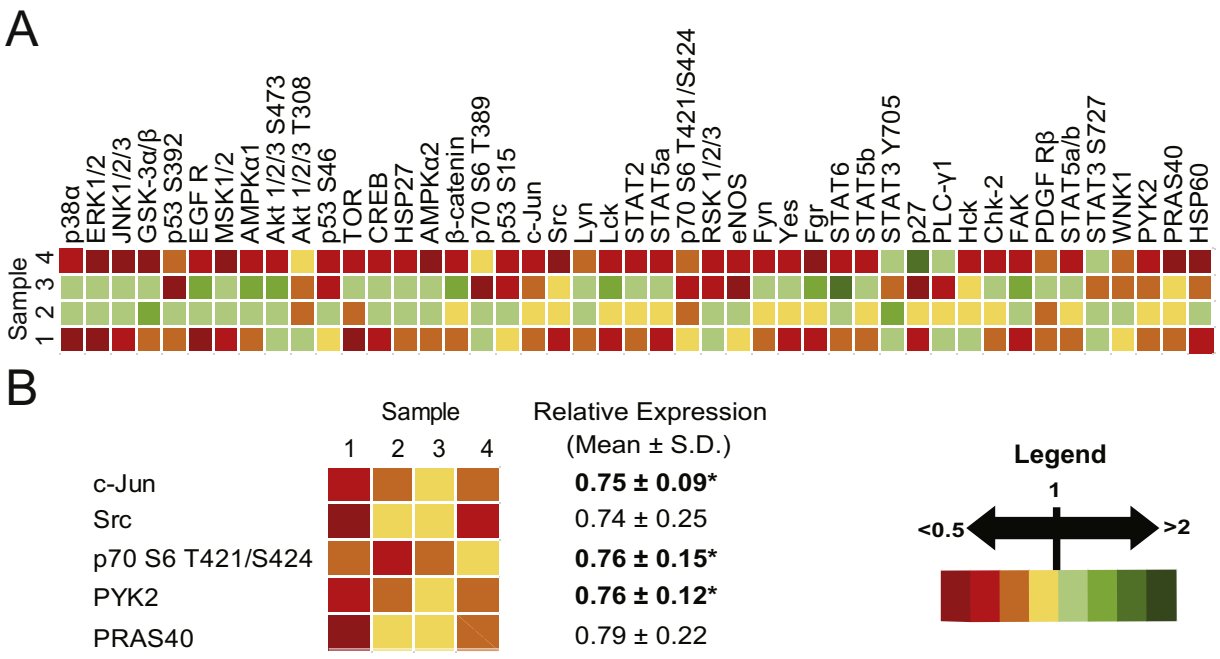

Fig. 6. (A) Expression of phosphorylated kinases associated with mitogen-activated protein kinase (MAPK) signaling in marrow cells. Each sample represents the expression of cells from a mechanically stimulated explant relative to a paired control explant from the same vertebra of the same animal. (B) Kinases that demonstrated consistent regulation across all samples, including their mean expression ± S.D. (*$p < 0.05$; One sample *t*-test).

decreased about 25% relative to controls in our study, and may have been sufficient to positively affect cyclin-D1 expression. Moreover, c-Jun phosphorylation was measured across multiple cell types, in which it may play different roles. For example, inhibition of the c-Jun pathway suppresses osteoclast differentiation, [60], and dominant negative c-Jun expression leads to osteopetrosis in mice [61]. Similarly, knocking out c-Jun in mouse macrophages reduces macrophage activation and subsequent inflammation, decreasing bone loss [62]. We did not measure the bone resorption rate or osteoclast numbers in this study. Hence it is unclear whether alterations in c-Jun phosphorylation affected bone resorption. We did not measure c-Jun gene expression in our experiments, because we were unable to find an effective PCR primer for the porcine gene. In any case, cyclin-D1 mRNA expression increased two-fold in stimulated explants suggesting that AP-1 was affected by bone marrow mechanotransduction.

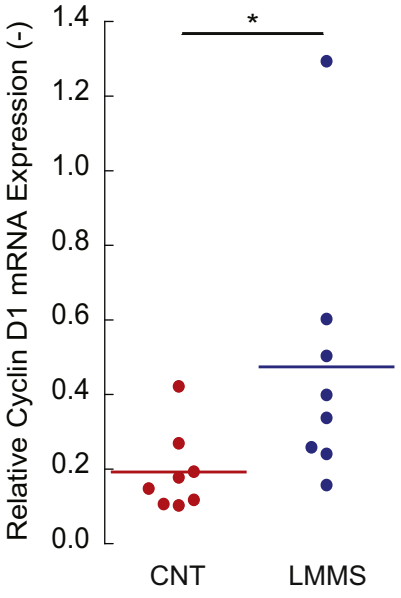

Fig. 7. Cyclin-D1 gene expression relative to RSP2 was higher in marrow cells from loaded explants compared to controls (*$p < 0.05$, Paired *t*-test). We verified that the outlier did not affect the result ($p = 0.011$).

The bioreactor culture system enabled the marrow to maintain its *in vivo* multicellular niche and location within the trabeculae of bone, as changes in microenvironment may affect stem cells in the marrow [63]. The explants remained viable throughout the 28 day study, as indicated by the presence of MSCs in the extracted marrow and double-labeled mineralizing bone surfaces, with similar mineral apposition rate and bone formation rate to previous *in vivo* studies of tibial loading in mice [64,65]. In addition, gene expression in osteocytes and marrow cells remained similar to Day 0 samples after bioreactor culture (see Supplementary data).

There are some limitations to this study. The effects of animal breed, age, and sex were not controlled. All of these may contribute to bone remodeling and likely affected the inter-sample variability. Sex-specific effects have been observed in porcine bone development [66]. However, the use of *in situ* tissue culture removed the bone and marrow from systemic hormones associated with sex, but genetic differences in different breeds likely increased the number of samples needed to attain significance. Harvesting the tissue may cause an inflammatory state, which may induce bone formation. However, the same process was applied across experimental conditions, so all explants were subject to this effect. Although we did not measure osteocyte viability after bioreactor culture, David et al. reported 60% osteocyte viability in bovine trabecular bone after 3 weeks of bioreactor culture [67]. Osteocyte apoptosis within the center of bovine bone cores cultured *ex vivo* was similar to that observed *in vivo* [68]. Osteocyte death may be responsible for the positive bone formation rate measured in unloaded explants, although osteocyte death would be assumed to be identical in both loaded and unloaded explants, and the bone formation rate was still significantly higher in loaded explants. Finally, post-culture processing of marrow cells may affect their gene expression, as trypsin and centrifugal force were used to separate the marrow from the bone. Enzymatic separation of bone from non-skeletal tissues has been reported to alter gene expression measurements [69]. To minimize this effect, samples were kept on ice during processing. Most importantly, sample preparation

was identical across conditions. However, the methods may be limited for genes and proteins that respond rapidly to mechanical stimuli.

Increased gene expression of cyclin-D1 in stimulated marrow may signify an increase in proliferating cells, as cyclin-D1 is required for cell cycle progression [47]. Cyclin-D1 may also play a role in osteogenesis, as its expression is reduced four-fold in unloaded mouse femora compared to normally loaded controls [22], while it increases in mechanically stimulated bone *in vivo* as well as in osteoblasts *in vitro* [70]. These studies suggest that mechanotransduction upregulates cyclin-D1 expression, which may have played a role in increased bone formation in this study.

The results complement recent studies on mechanotransduction in bone marrow. In addition to inducing bone formation [41], mechanical stimulation of marrow in explant culture downregulates primary cilia expression [42]. Transplantation of marrow from mice with genetically ablated primary cilia expression while maintaining wild type osteocytes decreased the bone formation response to *in vivo* whole bone loading [39]. Altered c-Fos gene transcription following mechanical stimulation of marrow complements a similar finding in isolated megakaryocytes following *in vivo* whole bone loading in mice [32]. Taken together, these data support the notion that marrow cells respond to mechanical cues, and that whole bone loading affects marrow cells at both the gene and protein levels.

The mineral apposition and bone formation rates we measured were higher than those in previous bioreactor studies. Human trabecular bone explants cultured for 28 days in Zetos bioreactors with and without mechanical loading had an average MAR of 0.256 μm/day and 0.003 μm/day, respectively, and BFR of 9.8 $\mu m^3/\mu m^2$/yr and 0.6 $\mu m^3/\mu m^2$/yr, respectively [71]. In contrast, bovine sternum trabecular bone explants cultured with and without mechanical stimulation at 300 cycles of 4000 με per day had an average MAR of 0.94 μm/day and 0.71 μm/day, respectively; which is comparable to our data [67]. Media in the Mann et al. study contained 1.5 and 4 times less AA2P and β-GP, respectively, than our study. Media in the David et al. did not contain β-GP and contained 5000 times less AA2P. As such, there is no clear trend in the effects of these supplements on bone formation.

Sclerostin expression in our study was similar to previous observations. Slightly over 70% of osteocytes were positive for sclerostin in human trabecular bone [25]. Similarly, approximately 60% of osteocytes were sclerostin positive in a study of rat hindlimb unloading, although there was nearly twice as much SOST gene transcription after 3 days of hind limb suspension compared with ground-loaded controls [7]. Low intensity vibration decreased SOST expression in osteocytes *in vitro* [72]. However, osteocytes embedded within mineralized matrix may experience less stress than osteocytes *in vitro*. Sclerostin expression was decreased in mouse trabecular bone after whole body vibration [73], but the acceleration applied was approximately 7 times higher than that used in this study. Further, whole body vibration may induce additional bone deformation due to muscular loads, while computational analyses suggest almost no bone deformation in our system [51]. We observed no change in osteocyte RANKL/OPG expression due to LMMS. Lau et al. observed a decrease in RANKL expression in MLO-Y4 cells exposed to low magnitude, high-frequency vibration [74]. However, You et al. observed an increase in RANKL and OPG and an overall decrease in RANKL/OPG in osteocytes exposed to oscillatory fluid flow [75]. It is possible that the combination of vibration and fluid shear may act through different pathways to differentially regulate the RANKL/OPG axis. There are, of course, other osteocyte genes that can affect bone formation, such as Dickkopf-related protein 1 (Dkk1) and secreted frizzled-related protein 1 (sFRP1). It is possible that expression of these molecules was altered by the mechanical signal in this experiment while IGF-1, SOST, Cyr61, and CTGF were not.

It is possible that the increased bone formation was due to dedifferentiation of bone lining cells. The highest shear stress in the marrow occurs on the bone surface during LMMS [42,51], and membrane deformation of bone lining cells and osteoblasts engages mechanically sensitive focal adhesions, ion channels, and adherin junctions, leading to activation of several kinase signaling cascades. For example, stretch-activated ion channels release internal calcium ions into osteoblasts, which can trigger Src, focal adhesion kinase (FAK), and MAP kinase activation [76]. Both Src and FAK have been shown to regulate mechanical signaling to influence MSC lineage commitment [77]. Additionally, strain can induce upregulation of mechanoregulatory genes, such as c-Fos and COX2 [76]. While c-Fos gene expression increased in the stimulated explants, COX2 did not, nor did we find increased activation of MAPK pathway proteins. However, osteoblasts and bone lining cells may be too few in number to have affected the proteome or mRNA of the whole marrow aliquots studied.

The application of explant culture provided a unique means to isolate the effects of loading to marrow cells in order to measure the response to mechanical loading. In comparison to *in vivo* models of bone adaptation, systemic effects were also minimized. This could be beneficial for studying osteogenic drugs and their interaction with bone [78]. In this model, only localized cell signaling in the bone is present. At the same time, the effects of paracrine signaling between the differing cell populations that affects the osteogenic response is maintained [79].

Acknowledgements

This material is based upon work supported by the National Science Foundation under Grant No. CMMI-1453467 and CMMI-1100207.

Appendix A. Supplementary data

Supplementary data to this article can be found online at https://doi.org/10.1016/j.bone.2017.11.007.

References

[1] J. Wolff, Das Gesetz der Transformation der Knochen, Verlag August Hirschwald, Berlin, Germany, 1892http://www.springer.com/us/book/9783642710339, Accessed date: 14 April 2017.
[2] H.M. Frost, Bone's mechanostat: a 2003 update, Anat. Rec. A: Discov. Mol. Cell. Evol. Biol. 275 (2003) 1081–1101, https://doi.org/10.1002/ar.a.10119.
[3] H.M. Frost, J.L. Ferretti, W.S. Jee, Perspectives: some roles of mechanical usage, muscle strength, and the mechanostat in skeletal physiology, disease, and research, Calcif. Tissue Int. 62 (1998) 1–7.
[4] J.C. Fritton, E.R. Myers, T.M. Wright, M.C.H. van der Meulen, Loading induces site-specific increases in mineral content assessed by microcomputed tomography of the mouse tibia, Bone 36 (2005) 1030–1038, https://doi.org/10.1016/j.bone.2005.02.013.
[5] B. Krølner, B. Toft, S. Pors Nielsen, E. Tøndevold, Physical exercise as prophylaxis against involutional vertebral bone loss: a controlled trial, Clin. Sci. (Lond.) 1979 (64) (1983) 541–546.
[6] M.C.H. van der Meulen, X. Yang, T.G. Morgan, M.P.G. Bostrom, The effects of loading on cancellous bone in the rabbit, Clin. Orthop. 467 (2009) 2000–2006, https://doi.org/10.1007/s11999-009-0897-4.
[7] A.G. Robling, P.J. Niziolek, L.A. Baldridge, K.W. Condon, M.R. Allen, I. Alam, S.M. Mantila, J. Gluhak-Heinrich, T.M. Bellido, S.E. Harris, C.H. Turner, Mechanical stimulation of bone in vivo reduces osteocyte expression of Sost/sclerostin, J. Biol. Chem. 283 (2008) 5866–5875, https://doi.org/10.1074/jbc.M705092200.
[8] C. Rubin, G. Xu, S. Judex, The anabolic activity of bone tissue, suppressed by disuse, is normalized by brief exposure to extremely low-magnitude mechanical stimuli, FASEB J. 15 (2001) 2225–2229, https://doi.org/10.1096/fj.01-0166com.
[9] M.J. Silva, M.D. Brodt, M.A. Lynch, A.L. Stephens, D.J. Wood, R. Civitelli, Tibial loading increases osteogenic gene expression and cortical bone volume in mature and middle-aged mice, PLoS One 7 (2012), e34980. https://doi.org/10.1371/journal.pone.0034980.
[10] J.I. Aguirre, L.I. Plotkin, S.A. Stewart, R.S. Weinstein, A.M. Parfitt, S.C. Manolagas, T. Bellido, Osteocyte apoptosis is induced by weightlessness in mice and precedes osteoclast recruitment and bone loss, J. Bone Miner. Res. Off. J. Am. Soc. Bone Miner. Res. 21 (2006) 605–615, https://doi.org/10.1359/jbmr.060107.
[11] K. Eimori, N. Endo, S. Uchiyama, Y. Takahashi, H. Kawashima, K. Watanabe, Disrupted bone metabolism in long-term bedridden patients, PLoS One 11 (2016)https://doi.org/10.1371/journal.pone.0156991.
[12] C.T. Rubin, L.E. Lanyon, Osteoregulatory nature of mechanical stimuli: function as a determinant for adaptive remodeling in bone, J. Orthop. Res. 5 (1987) 300–310, https://doi.org/10.1002/jor.1100050217.
[13] J.E. Zerwekh, L.A. Ruml, F. Gottschalk, C.Y. Pak, The effects of twelve weeks of bed rest on bone histology, biochemical markers of bone turnover, and calcium homeostasis in eleven normal subjects, J. Bone Miner. Res. Off. J. Am. Soc. Bone Miner. Res. 13 (1998) 1594–1601, https://doi.org/10.1359/jbmr.1998.13.10.1594.

[14] S. Weinbaum, S.C. Cowin, Y. Zeng, A model for the excitation of osteocytes by mechanical loading-induced bone fluid shear stresses, J. Biomech. 27 (1994) 339–360.
[15] L.F. Bonewald, The amazing osteocyte, J. Bone Miner. Res. Off. J. Am. Soc. Bone Miner. Res. 26 (2011) 229–238, https://doi.org/10.1002/jbmr.320.
[16] J. Klein-Nulend, P.J. Nijweide, E.H. Burger, Osteocyte and bone structure, Curr. Osteoporos. Rep. 1 (2003) 5–10.
[17] M.B. Schaffler, W.-Y. Cheung, R. Majeska, O. Kennedy, Osteocytes: master orchestrators of bone, Calcif. Tissue Int. 94 (2014) 5–24, https://doi.org/10.1007/s00223-013-9790-y.
[18] J.M. Lean, A.G. Mackay, J.W. Chow, T.J. Chambers, Osteocytic expression of mRNA for c-fos and IGF-I: an immediate early gene response to an osteogenic stimulus, Am. J. Phys. 270 (1996) E937–945.
[19] M.H.-C. Sheng, X.-D. Zhou, L.F. Bonewald, D.J. Baylink, K.-H.W. Lau, Disruption of the insulin-like growth factor-1 gene in osteocytes impairs developmental bone growth in mice, Bone 52 (2013) 133–144, https://doi.org/10.1016/j.bone.2012.09.027.
[20] M. Semënov, K. Tamai, X. He, SOST is a ligand for LRP5/LRP6 and a Wnt signaling inhibitor, J. Biol. Chem. 280 (2005) 26770–26775, https://doi.org/10.1074/jbc.M504308200.
[21] X. Li, M.S. Ominsky, Q.-T. Niu, N. Sun, B. Daugherty, D. D'Agostin, C. Kurahara, Y. Gao, J. Cao, J. Gong, F. Asuncion, M. Barrero, K. Warmington, D. Dwyer, M. Stolina, S. Morony, I. Sarosi, P.J. Kostenuik, D.L. Lacey, W.S. Simonet, H.Z. Ke, C. Paszty, Targeted deletion of the sclerostin gene in mice results in increased bone formation and bone strength, J. Bone Miner. Res. Off. J. Am. Soc. Bone Miner. Res. 23 (2008) 860–869, https://doi.org/10.1359/jbmr.080216.
[22] C. Lin, X. Jiang, Z. Dai, X. Guo, T. Weng, J. Wang, Y. Li, G. Feng, X. Gao, L. He, Sclerostin mediates bone response to mechanical unloading through antagonizing Wnt/beta-catenin signaling, J. Bone Miner. Res. Off. J. Am. Soc. Bone Miner. Res. 24 (2009) 1651–1661, https://doi.org/10.1359/jbmr.090411.
[23] X. Tu, Y. Rhee, K.W. Condon, N. Bivi, M.R. Allen, D. Dwyer, M. Stolina, C.H. Turner, A.G. Robling, L.I. Plotkin, T. Bellido, Sost downregulation and local Wnt signaling are required for the osteogenic response to mechanical loading, Bone 50 (2012) 209–217, https://doi.org/10.1016/j.bone.2011.10.025.
[24] D.G. Winkler, M.K. Sutherland, J.C. Geoghegan, C. Yu, T. Hayes, J.E. Skonier, D. Shpektor, M. Jonas, B.R. Kovacevich, K. Staehling-Hampton, M. Appleby, M.E. Brunkow, J.A. Latham, Osteocyte control of bone formation via sclerostin, a novel BMP antagonist, EMBO J. 22 (2003) 6267–6276, https://doi.org/10.1093/emboj/cdg599.
[25] K.E.S. Poole, R.L. van Bezooijen, N. Loveridge, H. Hamersma, S.E. Papapoulos, C.W. Löwik, J. Reeve, Sclerostin is a delayed secreted product of osteocytes that inhibits bone formation, FASEB J. 19 (2005) 1842–1844, https://doi.org/10.1096/fj.05-4221fje.
[26] C.H. Kim, L. You, C.E. Yellowley, C.R. Jacobs, Oscillatory fluid flow-induced shear stress decreases osteoclastogenesis through RANKL and OPG signaling, Bone 39 (2006) 1043–1047, https://doi.org/10.1016/j.bone.2006.05.017.
[27] J. Xiong, M. Piemontese, M. Onal, J. Campbell, J.J. Goellner, V. Dusevich, L. Bonewald, S.C. Manolagas, C.A. O'Brien, Osteocytes, not osteoblasts or lining cells, are the main source of the RANKL required for osteoclast formation in remodeling bone, PLoS One 10 (2015), e0138189. https://doi.org/10.1371/journal.pone.0138189.
[28] M. Piemontese, J. Xiong, Y. Fujiwara, J.D. Thostenson, C.A. O'Brien, Cortical bone loss caused by glucocorticoid excess requires RANKL production by osteocytes and is associated with reduced OPG expression in mice, Am. J. Physiol. Endocrinol. Metab. 311 (2016) E587–593, https://doi.org/10.1152/ajpendo.00219.2016.
[29] A.B. Castillo, C.R. Jacobs, Mesenchymal stem cell mechanobiology, Curr. Osteoporos. Rep. 8 (2010) 98–104, https://doi.org/10.1007/s11914-010-0015-2.
[30] R.C. Riddle, A.F. Taylor, J.R. Rogers, H.J. Donahue, ATP release mediates fluid flow-induced proliferation of human bone marrow stromal cells, J. Bone Miner. Res. Off. J. Am. Soc. Bone Miner. Res. 22 (2007) 589–600, https://doi.org/10.1359/jbmr.070113.
[31] R. Smalt, F.T. Mitchell, R.L. Howard, T.J. Chambers, Induction of NO and prostaglandin E2 in osteoblasts by wall-shear stress but not mechanical strain, Am. J. Physiol. Endocrinol. Metab. 273 (1997) E751–E758.
[32] C.P. Soves, J.D. Miller, D.L. Begun, R.S. Taichman, K.D. Hankenson, S.A. Goldstein, Megakaryocytes are mechanically responsive and influence osteoblast proliferation and differentiation, Bone 66 (2014) 111–120, https://doi.org/10.1016/j.bone.2014.05.015.
[33] T.A. Metzger, S.A. Schwaner, A.J. LaNeve, T.C. Kreipke, G.L. Niebur, Pressure and shear stress in trabecular bone marrow during whole bone loading, J. Biomech. 48 (2015) 3035–3043, https://doi.org/10.1016/j.jbiomech.2015.07.028.
[34] T.A. Metzger, T.C. Kreipke, T.J. Vaughan, L.M. McNamara, G.L. Niebur, The in situ mechanics of trabecular bone marrow: the potential for mechanobiological response, J. Biomech. Eng. 137 (2015)https://doi.org/10.1115/1.4028985.
[35] T.J. Vaughan, M. Voisin, G.L. Niebur, L.M. McNamara, Multiscale modeling of trabecular bone marrow: understanding the micromechanical environment of mesenchymal stem cells during osteoporosis, J. Biomech. Eng. 137 (2015)https://doi.org/10.1115/1.4028986.
[36] U.A. Gurkan, A. Krueger, O. Akkus, Ossifying bone marrow explant culture as a three-dimensional mechanoresponsive in vitro model of osteogenesis, Tissue Eng. Part A 17 (2010) 417–428, https://doi.org/10.1089/ten.tea.2010.0193.
[37] U.A. Gurkan, J. Gargac, O. Akkus, The sequential production profiles of growth factors and their relations to bone volume in ossifying bone marrow explants, Tissue Eng. Part A 16 (2010) 2295–2306, https://doi.org/10.1089/ten.TEA.2009.0565.
[38] U.A. Gurkan, R. Golden, V. Kishore, C.P. Riley, J. Adamec, O. Akkus, Immune and inflammatory pathways are involved in inherent bone marrow ossification, Clin. Orthop. 470 (2012) 2528–2540, https://doi.org/10.1007/s11999-012-2459-4.
[39] J.C. Chen, D.A. Hoey, M. Chua, R. Bellon, C.R. Jacobs, Mechanical signals promote osteogenic fate through a primary cilia-mediated mechanism, FASEB J. 30 (2016) 1504–1511, https://doi.org/10.1096/fj.15-276402.
[40] D. Webster, F.A. Schulte, F.M. Lambers, G. Kuhn, R. Müller, Strain energy density gradients in bone marrow predict osteoblast and osteoclast activity: a finite element study, J. Biomech. 48 (2015) 866–874, https://doi.org/10.1016/j.jbiomech.2014.12.009.
[41] E. Birmingham, T.C. Kreipke, E.B. Dolan, T.R. Coughlin, P. Owens, L.M. McNamara, G.L. Niebur, P.E. McHugh, Mechanical stimulation of bone marrow in situ induces bone formation in trabecular explants, Ann. Biomed. Eng. 43 (2014) 1036–1050, https://doi.org/10.1007/s10439-014-1135-0.
[42] T.R. Coughlin, J. Schiavi, M. Alyssa Varsanik, M. Voisin, E. Birmingham, M.G. Haugh, L.M. McNamara, G.L. Niebur, Primary cilia expression in bone marrow in response to mechanical stimulation in explant bioreactor culture, Eur. Cell. Mater. 32 (2016) 111–122.
[43] M.F. Pittenger, A.M. Mackay, S.C. Beck, R.K. Jaiswal, R. Douglas, J.D. Mosca, M.A. Moorman, D.W. Simonetti, S. Craig, D.R. Marshak, Multilineage potential of adult human mesenchymal stem cells, Science 284 (1999) 143–147, https://doi.org/10.1126/science.284.5411.143.
[44] A.M. Parfitt, M.K. Drezner, F.H. Glorieux, J.A. Kanis, H. Malluche, P.J. Meunier, S.M. Ott, R.R. Recker, Bone histomorphometry: standardization of nomenclature, symbols, and units. Report of the ASBMR Histomorphometry Nomenclature Committee, J. Bone Miner. Res. Off. J. Am. Soc. Bone Miner. Res. 2 (1987) 595–610, https://doi.org/10.1002/jbmr.5650020617.
[45] N.H. Kelly, J.C. Schimenti, F. Patrick Ross, M.C.H. van der Meulen, A method for isolating high quality RNA from mouse cortical and cancellous bone, Bone 68 (2014) 1–5, https://doi.org/10.1016/j.bone.2014.07.022.
[46] C.A. O'Brien, L.I. Plotkin, C. Galli, J.J. Goellner, A.R. Gortazar, M.R. Allen, A.G. Robling, M. Bouxsein, E. Schipani, C.H. Turner, R.L. Jilka, R.S. Weinstein, S.C. Manolagas, T. Bellido, Control of bone mass and remodeling by PTH receptor signaling in osteocytes, PLoS One 3 (2008)https://doi.org/10.1371/journal.pone.0002942.
[47] V. Baldin, J. Lukas, M.J. Marcote, M. Pagano, G. Draetta, Cyclin D1 is a nuclear protein required for cell cycle progression in G1, Genes Dev. 7 (1993) 812–821, https://doi.org/10.1101/gad.7.5.812.
[48] C.J. Sherr, Mammalian G1 cyclins, Cell 73 (1993) 1059–1065, https://doi.org/10.1016/0092-8674(93)90636-5.
[49] R. Sapir-Koren, G. Livshits, Osteocyte control of bone remodeling: is sclerostin a key molecular coordinator of the balanced bone resorption-formation cycles? Osteoporos. Int. J. Establ. Result Coop. Eur. Found. Osteoporos. Natl. Osteoporos. Found. USA. 25 (2014) 2685–2700, https://doi.org/10.1007/s00198-014-2808-0.
[50] X. Tu, J. Delgado-Calle, K.W. Condon, M. Maycas, H. Zhang, N. Carlesso, M.M. Taketo, D.B. Burr, L.I. Plotkin, T. Bellido, Osteocytes mediate the anabolic actions of canonical Wnt/β-catenin signaling in bone, Proc. Natl. Acad. Sci. U. S. A. 112 (2015) E478–486, https://doi.org/10.1073/pnas.1409857112.
[51] T.R. Coughlin, G.L. Niebur, Fluid shear stress in trabecular bone marrow due to low-magnitude high-frequency vibration, J. Biomech. 45 (2012) 2222–2229, https://doi.org/10.1016/j.jbiomech.2012.06.020.
[52] G. Uzer, W.R. Thompson, B. Sen, Z. Xie, S.S. Yen, S. Miller, G. Bas, M. Styner, C.T. Rubin, S. Judex, K. Burridge, J. Rubin, Cell Mechanosensitivity to extremely low-magnitude signals is enabled by a LINCed nucleus, Stem Cells Dayt. Ohio. 33 (2015) 2063–2076, https://doi.org/10.1002/stem.2004.
[53] E. Zhao, H. Xu, L. Wang, I. Kryczek, K. Wu, Y. Hu, G. Wang, W. Zou, Bone marrow and the control of immunity, Cell. Mol. Immunol. 9 (2012) 11–19, https://doi.org/10.1038/cmi.2011.47.
[54] P.P. Eleniste, V. Patel, S. Posritong, O. Zero, H. Largura, Y.-H. Cheng, E.R. Himes, M. Hamilton, J. Baughman, M.A. Kacena, A. Bruzzaniti, Pyk2 and megakaryocytes regulate osteoblast differentiation and migration via distinct and overlapping mechanisms, J. Cell. Biochem. 117 (2016) 1396–1406, https://doi.org/10.1002/jcb.25430.
[55] L. Buckbinder, D.T. Crawford, H. Qi, H.Z. Ke, L.M. Olson, K.R. Long, P.C. Bonnette, A.P. Baumann, J.E. Hambor, W.A. Grasser, L.C. Pan, T.A. Owen, M.J. Luzzio, C.A. Hulford, D.F. Gebhard, V.M. Paralkar, H.A. Simmons, J.C. Kath, W.G. Roberts, S.L. Smock, A. Guzman-Perez, T.A. Brown, M. Li, Proline-rich tyrosine kinase 2 regulates osteoprogenitor cells and bone formation, and offers an anabolic treatment approach for osteoporosis, Proc. Natl. Acad. Sci. U. S. A. 104 (2007) 10619–10624, https://doi.org/10.1073/pnas.0701421104.
[56] J.G. Allen, M.R. Lee, C.-Y.E. Han, J. Scherrer, S. Flynn, C. Boucher, H. Zhao, A.B. O'Connor, P. Roveto, D. Bauer, R. Graceffa, W.G. Richards, P. Babij, Identification of small molecule inhibitors of proline-rich tyrosine kinase 2 (Pyk2) with osteogenic activity in osteoblast cells, Bioorg. Med. Chem. Lett. 19 (2009) 4924–4928, https://doi.org/10.1016/j.bmcl.2009.07.084.
[57] P.C. Bonnette, B.S. Robinson, J.C. Silva, M.P. Stokes, A.D. Brosius, A. Baumann, L. Buckbinder, Phosphoproteomic characterization of PYK2 signaling pathways involved in osteogenesis, J. Proteome 73 (2010) 1306–1320, https://doi.org/10.1016/j.jprot.2010.01.011.
[58] R. Wisdom, R.S. Johnson, C. Moore, c-Jun regulates cell cycle progression and apoptosis by distinct mechanisms, EMBO J. 18 (1999) 188–197, https://doi.org/10.1093/emboj/18.1.188.
[59] L. Bakiri, D. Lallemand, E. Bossy-Wetzel, M. Yaniv, Cell cycle-dependent variations in c-Jun and JunB phosphorylation: a role in the control of cyclin D1 expression, EMBO J. 19 (2000) 2056–2068, https://doi.org/10.1093/emboj/19.9.2056.
[60] J.-P. David, K. Sabapathy, O. Hoffmann, M.H. Idarraga, E.F. Wagner, JNK1 modulates osteoclastogenesis through both c-Jun phosphorylation-dependent and -independent mechanisms, J. Cell Sci. 115 (2002) 4317–4325, https://doi.org/10.1242/jcs.00082.
[61] F. Ikeda, R. Nishimura, T. Matsubara, S. Tanaka, J. Inoue, S.V. Reddy, K. Hata, K. Yamashita, T. Hiraga, T. Watanabe, T. Kukita, K. Yoshioka, A. Rao, T. Yoneda, Critical

roles of c-Jun signaling in regulation of NFAT family and RANKL-regulated osteoclast differentiation, J. Clin. Invest. 114 (2004) 475–484, https://doi.org/10.1172/JCI19657.
[62] N. Hannemann, J. Jordan, S. Paul, S. Reid, H.-W. Baenkler, S. Sonnewald, T. Bäuerle, J. Vera, G. Schett, A. Bozec, The AP-1 transcription factor c-Jun promotes arthritis by regulating cyclooxygenase-2 and arginase-1 expression in macrophages, J. Immunol. 2017 (1950)https://doi.org/10.4049/jimmunol.1601330.
[63] U.A. Gurkan, O. Akkus, The mechanical environment of bone marrow: a review, Ann. Biomed. Eng. 36 (2008) 1978–1991, https://doi.org/10.1007/s10439-008-9577-x.
[64] R. Garman, G. Gaudette, L.-R. Donahue, C. Rubin, S. Judex, Low-level accelerations applied in the absence of weight bearing can enhance trabecular bone formation, J. Orthop. Res. 25 (2007) 732–740, https://doi.org/10.1002/jor.20354.
[65] L. Xie, J.M. Jacobson, E.S. Choi, B. Busa, L.R. Donahue, L.M. Miller, C.T. Rubin, S. Judex, Low-level mechanical vibrations can influence bone resorption and bone formation in the growing skeleton, Bone 39 (2006) 1059–1066, https://doi.org/10.1016/j.bone.2006.05.012.
[66] V.L. Flöter, G. Galateanu, R.W. Fürst, D. Seidlová-Wuttke, W. Wuttke, E. Möstl, T.B. Hildebrandt, S.E. Ulbrich, Sex-specific effects of low-dose gestational estradiol-17β exposure on bone development in porcine offspring, Toxicology 366–367 (2016) 60–67, https://doi.org/10.1016/j.tox.2016.07.012.
[67] V. David, A. Guignandon, A. Martin, L. Malaval, M.-H. Lafage-Proust, A. Rattner, V. Mann, B. Noble, D.B. Jones, L. Vico, Ex vivo bone formation in bovine trabecular bone cultured in a dynamic 3D bioreactor is enhanced by compressive mechanical strain, Tissue Eng. Part A 14 (2008) 117–126, https://doi.org/10.1089/ten.a.2007.0051.
[68] J. Vivanco, S. Garcia, H.L. Ploeg, G. Alvarez, D. Cullen, E.L. Smith, Apparent elastic modulus of ex vivo trabecular bovine bone increases with dynamic loading, Proc. Inst. Mech. Eng. H 227 (2013) 904–912, https://doi.org/10.1177/0954411913486855.
[69] U.M. Ayturk, C.M. Jacobsen, D.C. Christodoulou, J. Gorham, J.G. Seidman, C.E. Seidman, A.G. Robling, M.L. Warman, An RNA-seq protocol to identify mRNA expression changes in mouse diaphyseal bone: applications in mice with bone property altering Lrp5 mutations, J. Bone Miner. Res. Off. J. Am. Soc. Bone Miner. Res. 28 (2013) 2081–2093, https://doi.org/10.1002/jbmr.1946.
[70] J.A. Robinson, M. Chatterjee-Kishore, P.J. Yaworsky, D.M. Cullen, W. Zhao, C. Li, Y. Kharode, L. Sauter, P. Babij, E.L. Brown, A.A. Hill, M.P. Akhter, M.L. Johnson, R.R. Recker, B.S. Komm, F.J. Bex, Wnt/β-catenin signaling is a normal physiological response to mechanical loading in bone, J. Biol. Chem. 281 (2006) 31720–31728, https://doi.org/10.1074/jbc.M602308200.
[71] V. Mann, C. Huber, G. Kogianni, D. Jones, B. Noble, The influence of mechanical stimulation on osteocyte apoptosis and bone viability in human trabecular bone, J. Musculoskelet. Neuronal Interact. 6 (2006) 408–417.
[72] W.R. Thompson, G. Uzer, K.E. Brobst, Z. Xie, B. Sen, S.S. Yen, M. Styner, J. Rubin, Osteocyte specific responses to soluble and mechanical stimuli in a stem cell derived culture model, Sci. Rep. 5 (2015), 11049. https://doi.org/10.1038/srep11049.
[73] V. Gnyubkin, A. Guignandon, N. Laroche, A. Vanden-Bossche, L. Malaval, L. Vico, High-acceleration whole body vibration stimulates cortical bone accrual and increases bone mineral content in growing mice, J. Biomech. 49 (2016) 1899–1908, https://doi.org/10.1016/j.jbiomech.2016.04.031.
[74] E. Lau, S. Al-Dujaili, A. Guenther, D. Liu, L. Wang, L. You, Effect of low-magnitude, high-frequency vibration on osteocytes in the regulation of osteoclasts, Bone 46 (2010) 1508–1515, https://doi.org/10.1016/j.bone.2010.02.031.
[75] L. You, S. Temiyasathit, P. Lee, C.H. Kim, P. Tummala, W. Yao, W. Kingery, A.M. Malone, R.Y. Kwon, C.R. Jacobs, Osteocytes as mechanosensors in the inhibition of bone resorption due to mechanical loading, Bone 42 (2008) 172–179, https://doi.org/10.1016/j.bone.2007.09.047.
[76] F.M. Pavalko, S.M. Norvell, D.B. Burr, C.H. Turner, R.L. Duncan, J.P. Bidwell, A model for mechanotransduction in bone cells: the load-bearing mechanosomes, J. Cell. Biochem. 88 (2003) 104–112, https://doi.org/10.1002/jcb.10284.
[77] W.R. Thompson, C. Guilluy, Z. Xie, B. Sen, K.E. Brobst, S.S. Yen, G. Uzer, M. Styner, N. Case, K. Burridge, J. Rubin, Mechanically activated Fyn utilizes mTORC2 to regulate RhoA and adipogenesis in mesenchymal stem cells, Stem Cells Dayt. Ohio. 31 (2013) 2528–2537, https://doi.org/10.1002/stem.1476.
[78] L.A. Meyer, M.G. Johnson, D.M. Cullen, J.F. Vivanco, R.D. Blank, H.-L. Ploeg, E.L. Smith, Combined exposure to big endothelin-1 and mechanical loading in bovine sternal cores promotes osteogenesis, Bone 85 (2016) 115–122, https://doi.org/10.1016/j.bone.2016.02.001.
[79] E. Birmingham, G.L. Niebur, P.E. McHugh, G. Shaw, F.P. Barry, L.M. McNamara, Osteogenic differentiation of mesenchymal stem cells is regulated by osteocyte and osteoblast cells in a simplified bone niche, Eur. Cell. Mater. 23 (2012) 13–27.